

Supporting Information

Electric Field-induced switching among multiple conductance pathways in single-molecule junctions

Tengyang Gao,^a Zhichao Pan,^a Zhuanyun Cai,^a Jueting Zheng,^a Chun Tang,^a Saisai Yuan,^a Shi qiang Zhao,^a Hua Bai,^b Yang Yang,^a Jia Shi,^a Zongyuan Xiao,^{*a} Junyang Liu^{*a} and Wenjing Hong^{*a}

^aState Key Laboratory of Physical Chemistry of Solid Surfaces, College of Chemistry and Chemical Engineering, Xiamen University, Xiamen 361005, China

^bCollege of Materials, Xiamen University, Xiamen 361005, China

Table of Contents

1. General information and molecular characterization
2. STM-BJ measurement and data analysis
3. Theoretical calculations
4. References

1. General information and molecular characterization

The 1, 4-Diaminobenzene (BDA, 99%) molecule was purchased from Sigma-Aldrich. The N1-phenylbenzene-1,4-diamine (PBDA, 98%) molecule was purchased from Aladdin. Ethanol (EtOH, 99.5%) and Hydrochloric acid (HCl, 36%) were purchased from Sinopharm Chemical Reagent Co., Ltd. The propylene carbonate (PC, 99.7%) was purchased from Sigma- Aldrich as a reagent without further purification.

Prepared the insulated gold tips: The gold wire was firstly etched using the electrochemical method in a 1:1 (v/v) mixture of 37% HCl and EtOH, then the gold tips were coated with wax in the heating condition.

ATAT was synthesized according to literature procedures, and its ^1H NMR (400.1 MHz, DMSO-d_6) spectrum matched reported data.^[1]

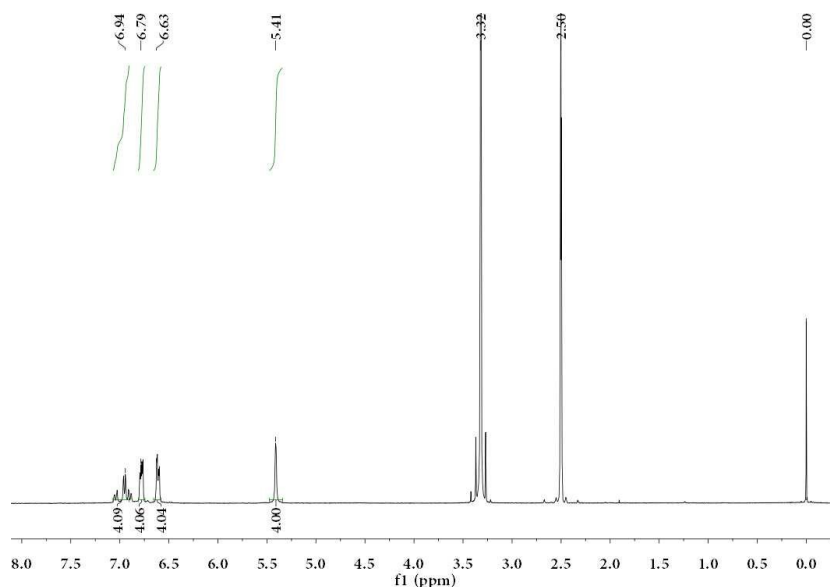


Fig. S1. ^1H NMR spectrum of ATAT in DMSO-d_6 .

2. STM-BJ measurement and data analysis

Our home-built STM-BJ setup was used to measure the molecular conductance between the tip and the substrate, a gold wire with 0.25 mm diameter was electrochemically etched as the tip, and the substrate was prepared by evaporating a 200 nm gold film on a silicon wafer. 1 mM solutions of ATAT, 1, 4-benzenediamine and N1-phenylbenzene-1,4-diamine (named as BDA and PBDA, used for control experiment) molecules were prepared separately in a propylene carbonate (PC) solvent. The etched gold tip was insulated with wax in order to reduce the tunneling background. The single-molecule conductance was measured, forming and breaking the molecular junction when the STM tip was repeatedly moved vertically and out of contact with the gold surface. Typical conductance-distance traces were measured with a sampling rate of 50 kHz. All the conductance traces were used for analysis without data selection. For each one-dimensional (1D) conductance histogram and two-dimensional (2D) conductance-distance histogram, at least one thousand individual curves were collected.

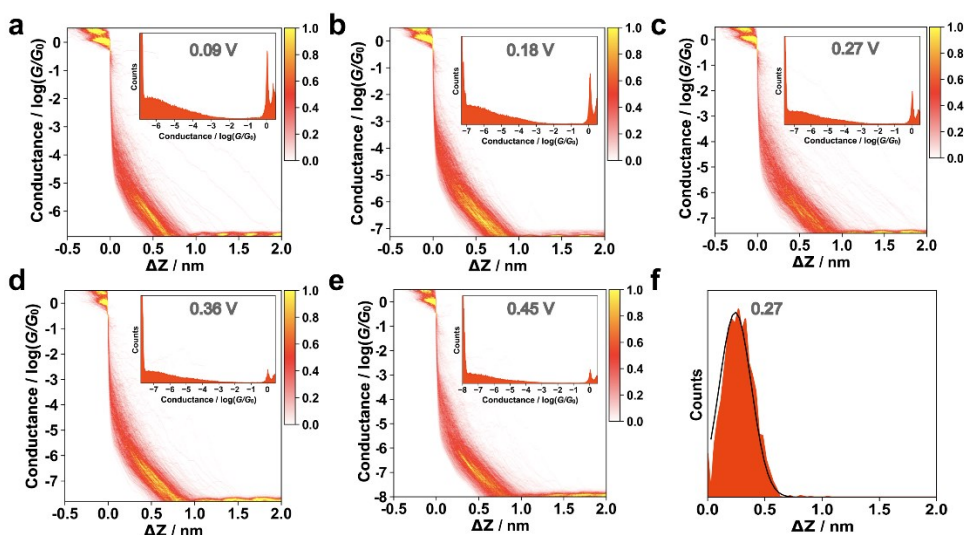


Fig. S2. 1D conductance histogram and 2D conductance-distance histogram for pure solvent under each bias condition. a) 0.09 V, b) 0.18 V, c) 0.27 V, d) 0.36 V and e) 0.45 V. No conductance junction was observed for pure PC. f) The relative displacement distribution histogram determined from the conductance range from $10^{3.5} G_0$ to $10^{-5} G_0$.

In the pure solvent without target molecules, we got the clean background under each bias voltage condition (0.09 V, 0.18 V, 0.27 V, 0.36 V, and 0.45 V), suggesting gold electrodes were clean during the experiment with pure solvent. By applying the tunneling decay constant of $\log(G/G_0)/\Delta z = -5.5 \text{ nm}^{-1}$, we calibrated stretching rate to make the relative displacement (Δz) in the conductance region of $10^{-3.5}$ to $10^{-5} G_0$ (24.8 nS to 0.775 nS) be $\sim 0.27 \text{ nm}$ ($-1.5/-5.5 = \sim 0.27 \text{ nm}$), the results were as shown in Fig. S2.

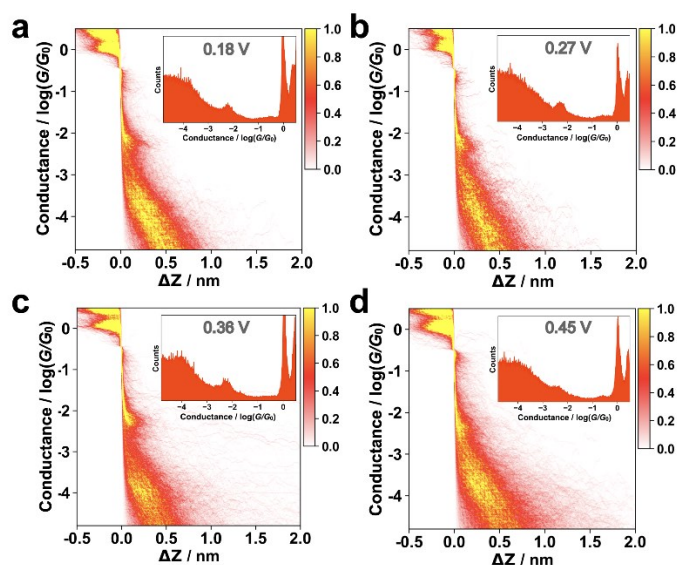


Fig. S3. 2D conductance histograms for BDA molecule under the bias range from 0.18 V to 0.45 V were shown in a), b), c), and d), respectively. 2D histograms are showing the conductance position at around $10^{-1.5} G_0$ to $10^{-2.5} G_0$ (2449 nS to 244.9 nS) and $10^{-3.5} G_0$ to $10^{-4.5} G_0$ (24.5 nS to 2.45 nS), which were very similar in appearance to the bias under 0.09 V and 0.45 V.

A high conductance position at around $10^{-1.5} G_0$ to $10^{-2.5} G_0$ (2449 nS to 244.9 nS), which could be ascribed to the single BDA molecule bonded to each electrode. At the same time, a low conductance appeared bonded to each electrode. While a low conductance appeared around $10^{-3.5} G_0$ to $10^{-4.5} G_0$ (24.5 nS to 2.45 nS) at all biases, the plateau length beyond a single-BDA junctions from the 2D conductance histograms as shown in Fig. S3, indicated that the electron transport through two molecules via hydrogen bond or interaction between terminal amino or benzene ring, which were in agreement with previous reports.^[2] Similarly, the PBDA molecule has the same phenomenon as the BDA molecule.

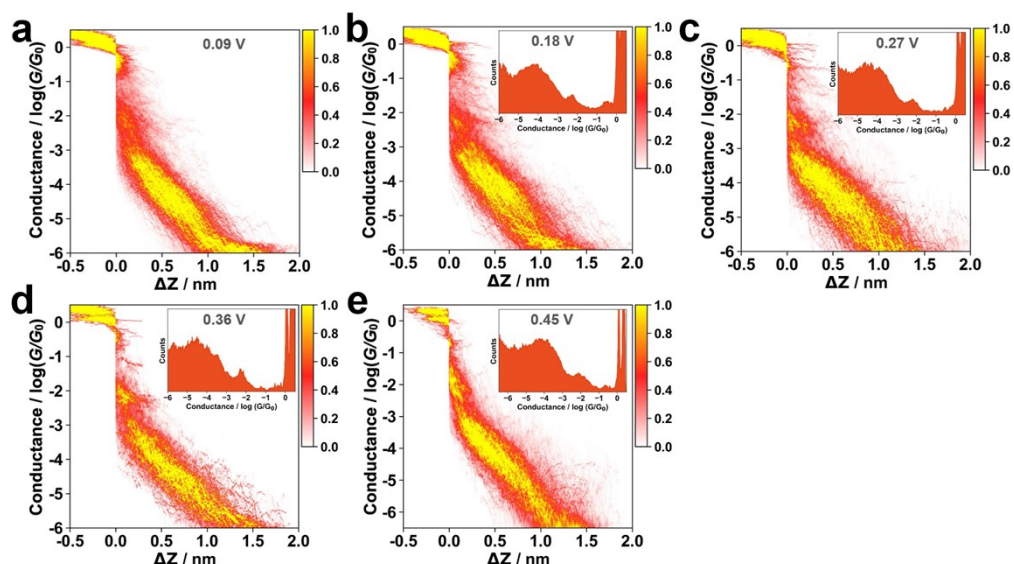


Fig. S4. 2D conductance histograms for PBDA molecule under the bias range from 0.09 V to 0.45 V were shown in a), b), c), d) and e), respectively. 2D histograms are showing the conductance position at around $10^{-1.5} G_0$ to $10^{-2.5} G_0$ (2449 nS to 244.9 nS) and $10^{-3.0} G_0$ to $10^{-5.0} G_0$ (77.5 nS to 0.775 nS), which were very similar in appearance to the bias under 0.09 V and 0.45 V.

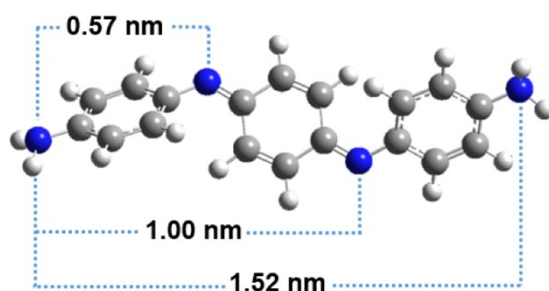


Fig. S5. The DFT length of the optimized molecular structure. Density functional theory (DFT) calculations were performed to optimize the structures for ATAT, with B3LYP functional and 6-311+G (d, p) basis sets in Gaussian 09 software package,^[3] the molecular geometry was relaxed and optimized until all force components on every atom was smaller than 10^{-2} eV/Å.

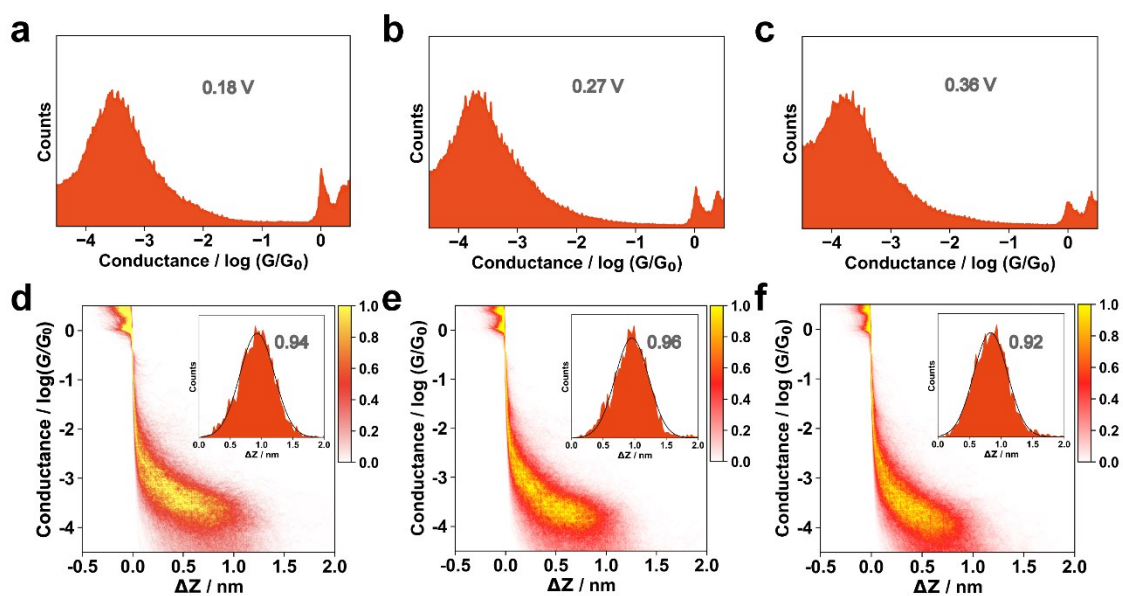


Fig. S6. One-dimensional (1D) semi-log conductance histograms under biases range from 0.18 V to 0.36 V were shown in a),b) and c), respectively. Corresponding 2D conductance histograms were shown in d),e) and f), respectively. The inset maps show the conductance versus displacement trace.

To correlate the conductance and the distance between the two electrodes for conductance feature, a 2D conductance-distance histogram was constructed from all of the traces. Under the bias between 0.09 V and 0.36 V, one prominent conductance cloud were found. The length was defined as the distance between the points where the conductance was located at the region of $10^{0.3}$ to $10^{4.3} G_0$ (38750 nS to 3.88 nS). All the plateau lengths were obtained by Gaussian fitting.

The Clustering method: To classify the multiple molecular conductance in the region $10^{-1.5}$ to $10^{-2.5} G_0$ (2449 nS to 245 nS) which could be overlapped, we performed clustering analysis using spectral clustering algorithm (since conductance curves are high dimensional data which cannot be clustered well by other classical clustering methods such as K-Means). Accurately, we followed the clustering routine provided by *sklearn*, a third party python module for machine learning. Similarity matrix of 1D conductance histograms (frequency distributions) in the region of interest (ROI, $10^{-1.5}$ to $10^{-2.5} G_0$) were used as inputs. Conductance traces were clustered into two classes, i.e., the HC cluster and the MC cluster, the corresponding 2D histogram for each class are shown in the main text (Fig. 2b).

Similarly, at a bias voltage of 0.45 V, the displacement distributions were obtained from the different regions after successfully separating the multiple molecular conductance. The conductance fell in between $10^{-2.5}$ and $10^{-4.3} G_0$ (245 nS and 3.88 nS) as the boundary for analyzing LC plateau length, the region of $10^{-0.3}$ to $10^{-2.5} G_0$ (38750 nS to 245 nS) was used for analyzing HC and MC plateau length, respectively. All the plateau lengths were obtained by Gaussian fitting.

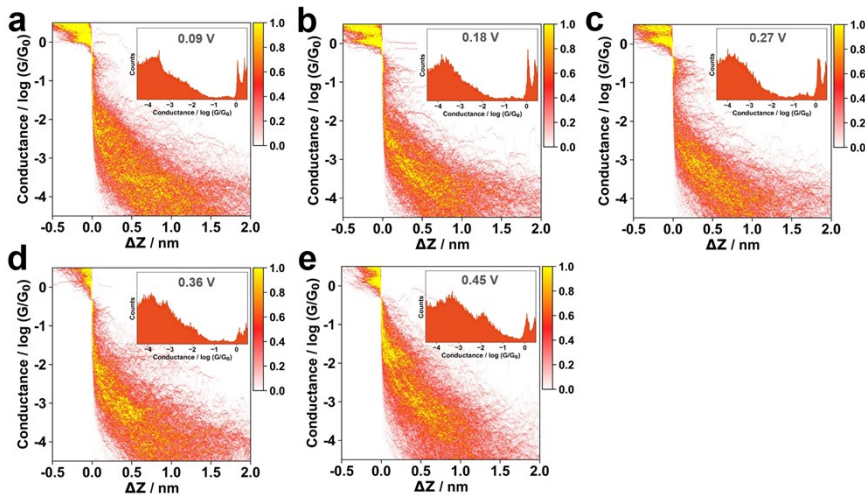


Fig. S7. 2D conductance histograms for ATAT (0.1 mM) under the bias between 0.09 V to 0.45 V were shown in a), b), c), d) and e), inset image is corresponding 1D histograms.

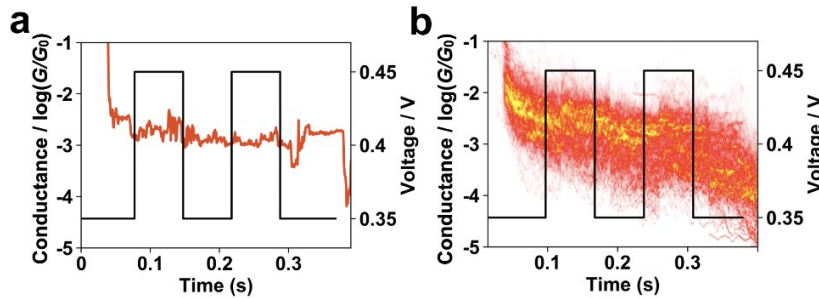


Fig. S8. Applied square-wave bias (black line) and conductance-time histograms acquired during a modified STM-BJ measurement where the junctions are held for 0.3 s: a) A typical individual curve of the no switch state and b) 2D conductance-time histogram constructed from corresponding individual curve. Of these, 71.2 % (141 out of 198) were in a no-switch state.

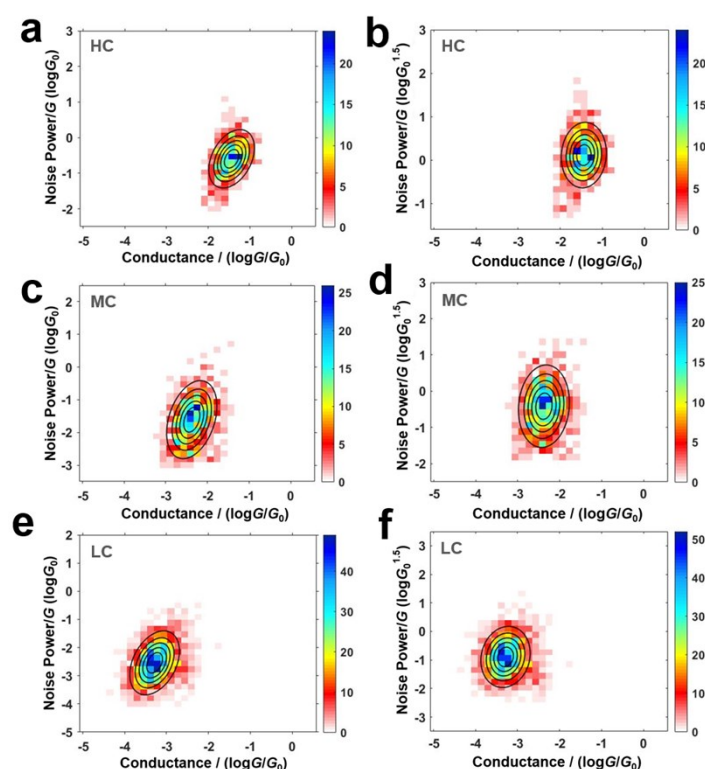


Fig. S9. 2D histograms of normalized flicker noise power versus average conductance for ATAT at 0.45 V. a) HC state and b) corresponding noise power scales as 1.5. c) MC state and d) corresponding noise power scales as 1.5. e) LC state and f) corresponding noise power scales as 1.5.

3. Theoretical calculations

To have a further insight into the conductance trend of the ATAT molecule, the transmission spectrum was calculated using a non-equilibrium Green's functions in the first-principle ATK package.^[4] We use the 6x6 gold slabs in the gold (111) crystal face with gold pyramids modeling the tip and the substrate, then the molecule binds to two electrodes to simulate the metal-molecule-metal system, and sets the k point with a grid of (3 *3 *301). The generalized gradient approximation (GGA) of the exchange and correlation functional is used with the Perdew-Burke-Ernzerhof parameterization (PBE), the single-zeta polarized (SZP) basis set was employed for Au atoms and the double-zeta polarized (DZP) basis sets were used for other atoms.^[5] The molecular junction structures were relaxed with a residual forces threshold value of 0.02 eV/Å, with the Au atoms kept fixed. All nitrogen atoms had the chance to attach to the Au electrode. Therefore, we built three junctions geometries, which are 1,2-position ATAT, 1,3-position ATAT and 1,4-position ATAT, except for the large steric hindrance of 2,3-position, as shown in main text Fig. 4c, and calculate the Landauer transmission across these junctions.^[6]

To evaluate the stability of molecular junctions under different electric fields, the molecular energy was calculated with a range of the field strengths from 0 to +0.008 a.u. The electric field was defined in Gaussian 09 software, the geometry optimization and calculation of molecular energy was carried out using B3LYP functional with dispersion correction and 6-311+G(d, p) standard basis sets. 6-311+G(d,p) basis group was used for C, N, and H atoms, and the LANL2DZ pseudopotential basis group was used for Au atoms. We fixed the Au atoms and applied 0.000 a.u., 0.002 a.u., 0.004 a.u., 0.006 a.u. and 0.008 a.u. electric fields in the direction of the Au atoms at both ends, using the same functional and basis groups for optimization.^[7] The molecular geometry was relaxed and optimized until all force components on every atom was smaller than 10^{-2} eV/Å, and the theoretical model as shown in Fig. S10.^[8]



Fig. S10. The models of different anchoring positions used for molecular energy calculation.

4. References

- [1] Y. Wei, C. Yang, T. Ding, *Tetrahedron Lett.* **1996**, *37*, 731-734.
- [2] T. Kim, H. Vázquez, M. S. Hybertsen, L. Venkataraman, *Nano Lett.* **2013**, *13*, 3358-3364.
- [3] A. D. Becke, *J. Chem. Phys.* **1993**, *98*, 5648-5652.
- [4] S. R. Bahn, K. W. Jacobsen, *Comput. Sci. Eng.* **2002**, *4*, 56-66.
- [5] a) M. Brandbyge, J. L. Mozos, P. Ordejon, J. Taylor, K. Stokbro, *Physical Review B* **2002**, *65*, 165401; b) J. Taylor, H. Guo, J. Wang, *Physical Review B* **2001**, *63*, 303-306.
- [6] R. Landauer, *J. Res. Dev.* **1957**, *1*, 223-231.
- [7] Z. Wang, D. Danovich, R. Ramanan, S. Shaik, *J. Am. Chem. Soc.* **2018**, *140*, 13350-13359.
- [8] M. Kiguchi, T. Ohto, S. Fujii, K. Sugiyasu, S. Nakajima, M. Takeuchi, H. Nakamura, *J. Am. Chem. Soc.* **2014**, *136*, 7327-7332.